Solar and Stellar Flares and Their Effects on Planets
Proceedings IAU Symposium No. 320, 2015
A.G. Kosovichev, S.L. Hawley, P. Heinzel

DOI: 00.0000/X000000000000000X

Multitemperature analysis of solar flare observed on 2003 March 29

Anna Kepa[1], Barbara Sylwester[1], Janusz Sylwester[1], Marek Siarkowski[1], Tomasz Mrozek[1,2], and Magdalena Gryciuk[1,2]

[1]Space Research Centre, Polish Academy of Sciences, Solar Physics Division, Wroclaw, Poland
email: ak@cbk.pan.wroc.pl

[2]Astronomical Institute, University of Wroclaw, Wroclaw, Poland

Abstract. We present results of multitemperature analysis of *GOES* C7.2 class flare SOL2003-03-29T10:15. This event occurred close to the centre of the solar disk and had two maxima in soft X-rays. We have performed analysis of physical parameters characterizing evolution of conditions in the flaring plasma. The temperature diagnostics have been carried out using the differential emission measure (DEM) approach based on the soft X-ray spectra collected by RESIK Bragg spectrometer. Analysis of data obtained by *RHESSI* provided opportunity to estimate the volume and thus calculating the density and thermal energy content of hot flaring plasma.

Keywords. Solar flares, spectra, differential emission measure

1. Introduction

During the RESIK experiment (Sylwester et al., 2005) onboard the *CORONAS-F* satellite several thousand of X-ray spectra in the wavelength range from 3.3 to 6.5 Å were obtained. The measurements include spectra of solar flares, active regions and quiet corona. The analysis of selected lines intensities allows the study of physical conditions in solar plasma. In this paper we focus our attentions on determinations and analysis of differential emission measure (DEM $\equiv \varphi(T_e)$) distributions, which is defined as follows: $\varphi(T_e) = N_e^2 \frac{dV}{dT_e}$ (N_e - electron density, V - plasma volume, T_e - temperature). The DEM convolved with the theoretically determined emission function ($f(T_e)$) of each selected wavelength gives the observed flux in appropriate spectral line/band i.

$$F_i = A_i \int_0^\infty f_i(T_e)\varphi(T_e)\, dT_e \qquad\qquad i = 1, 2, ...N \qquad (1.1)$$

where: A_i represents the assumed abundance of an element contributing to the flux of a particular line or spectral interval and N is the number of spectral bands used. The reconstruction of the DEM from measured line fluxes is based on the inversion of the set of integral equations 1.1 for N selected lines bands. To obtain a reliable DEM a set of lines with emission functions widely distributed over the temperature interval is required. Unfortunately a direct inversion of the data does not produce a unique DEM solution and additional constraints are needed to achieve a stable solution of this ill-posed inverse problem. There are a number of existing algorithms for reconstructing DEMs from solar and stellar data (e.g. Sylwester et al., 1980; Aschwanden et al., 2015). In this contribution we present (for the first time) the differential emission measure distributions obtained based on RESIK spectra using the Adaptive Differential Evolution method.

2. Observations and analysis

We present results of analysis of C7.2 flare SOL2003-03-29T10:15 observed by RESIK. The flux from *GOES* shows that the flare is complex and consists of a number of successive individual flares. Using elementary soft X-ray flare temporal profile we selected 6 individual flares composing *GOES lightcurve* (Figure 1, left; Gryciuk et al., 2015).

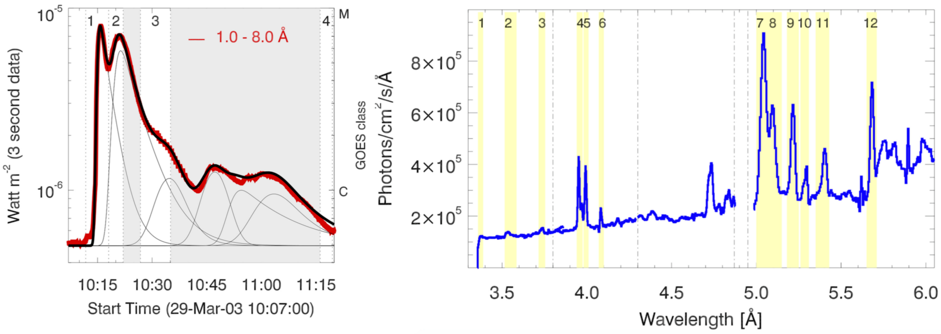

Figure 1. Left: *GOES* 1 - 8 Å lightcurve (in red) with optimal fit of elementary flares (thin black lines). The thick black line represents the sum of individual overlapped flare profiles. The grey strips indicate time intervals of passages through a polar van Allen radiation belt when the RESIK high-voltages were turned off and no observations were made. The four numbers denote intervals over which RESIK spectra were integrated for DEM analysis. Right: Average RESIK spectrum (integrated over 24 min) for SOL2003-03-29T10:15 flare. The lines used in the analysis are marked (see Table 1 for the details). The dashed lines limit the four RESIK channels bands. Unfortunately, due to technical problems during this flare, channel 3 data are not reliable for the analysis.

Table 1. Spectral bands used to calculate the DEM distributions.

No.	Wavelength range [Å]	Main line	Channel
1	3.358 - 3.388	Ar XVII 3p	1
2	3.515 - 3.585	K XVIII (w)	1
3	3.715 - 3.754	Ar XVIII 2p	1
4	3.940 - 3.975	Ar XVII (w)	2
5	3.980 - 4.010	Ar XVII (z)	2
6	4.070 - 4.100	S XV 4p	2
7	5.000 - 5.075	S XV 2p (w)	4
8	5.075 - 5.150	S XV 2p (z)	4
9	5.180 - 5.250	Si XIV 3p	4
10	5.260 - 5.310	Si XIII 5p	4
11	5.350 - 5.430	Si XIII 4p	4
12	5.650 - 5.710	Si XIII 3p	4

For four selected time intervals (corresponding to different flares) we calculated the mean spectrum and fluxes in $N = 12$ wavelength ranges (Table 1). To avoid the contribution of non-flaring plasma, the preflare X-ray fluxes have been subtracted.

DEM determinations were made using Adaptive Differential Evolution method (genetic algorithm). Differential evolution, introduced by Storn, & Price (1997) is simple but powerful evolutionary algorithm for global optimization. Starting from randomly chosen initial populations of different DEMs a new generation of DEMs is produced by crossover and mutations. Our population had 100 individual DEM distributions or 'chromosomes'. Each chromosome consists of 100 gens. They correspond to DEM values for 100 temperatures in the range from 2 to 30 MK. Process of breeding (and multiplication) of the whole population is controlled by assumed fitness criterion based on the values of observed to calculated fluxes. Based on the actual DEM distribution the predicted flux was calculated using the formula 1.1. For chlorine abundance we adopted $A_{Cl} = 5.62 \times 10^{-7}$. For silicon, sulfur, argon, and potassium we used abundances calculated using the multithermal assumption (AbuOpt method; Sylwester et al., 2015). We assumed $A_{Si} = 2.618 \times 10^{-5}$, $A_S = 7.413 \times 10^{-6}$, $A_{Ar} = 3.083 \times 10^{-6}$, $A_K = 6.067 \times 10^{-7}$. For other elements we adopted abundances called as sun_coronal_ext.abund (available in the CHIANTI package). The process of evolution was stopped after 6000 generations, when the convergence became very slow. The minimum χ^2 values were in the range 1.5 - 2.3. The process of evolution was repeated 10 times, each time starting from a new random population. Ten of the best DEM distributions obtained for individual intervals are presented in Figure 2.

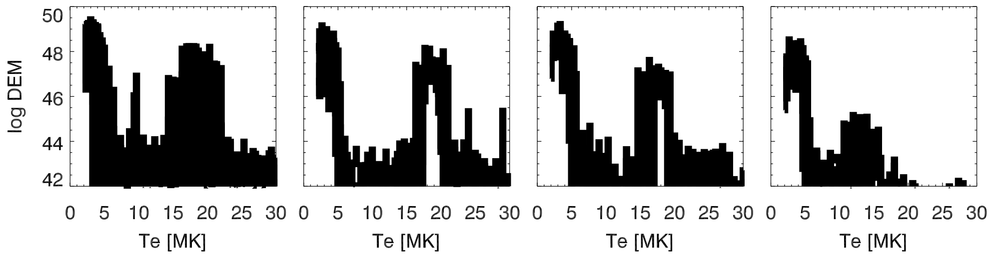

Figure 2. The DEM distributions obtained for individual intervals defined in Figure 1.

For the maximum and decay phase of the first flare the hard X-ray measurements from *RHESSI* were available. *RHESSI* images were obtained with the PIXON algorithm in the energy range 6 - 8 keV. From this data we estimated volumes (spherical shape was assumed). The spatial dimensions combined with the total emission measure of the hotter component allowed to estimate the electron density and thermal energy content.

3. Conclusion

For the first time we present the DEM distributions calculated using the Adaptive Differential Evolution method. Our DEM distributions are two components, which is consistent with previous results obtained using Withbroe-Sylwester method. The cooler component corresponds to plasma from 3 MK to 10 MK, hotter conforms the temperature range 12 - 25 MK. For the first flare the average volume (estimated from *RHESSI* data) is 1.9×10^{25} cm^3. This leads to the following values of electron density and thermal energy content for the hot component of the plasma: 2.9×10^{11} cm^{-3} as 4.11×10^{28} erg.

Acknowledgements

This research has been supported by Polish National Science Centre grants No. DEC-2013/09/N/ST9/02209, 2011/01/M/ST9/05878, and 2011/01/M/ST9/06096.

References

Aschwanden, M. J., Boerner, P., Caspi, A., McTiernan, J. M., Ryan, D., & Warren, H. P. 2015, *Sol. Phys.* (in press)
Gryciuk, M., Siarkowski, M., Gburek, S. at al. 2015, in preparation
Storn, R., & and Price, K. 1997, *Journal of Global Optimization*, 11, 341
Sylwester, B., Phillips, K.J.H., Sylwester, J., & Kepa, A. 2015, *ApJ*, 805, 49
Sylwester, J., Gaicki, I., Kordylewski Z. at al. 2005, *Sol. Phys.*, 226, 45
Sylwester, J., Schrijver, J., & Mewe, R. 1980, *Sol. Phys.*, 67, 285